Supplemental Material

# Bacterial Hen1 is a 3' terminal RNA ribose 2'O-methyltransferase component of a bacterial RNA repair cassette

Ruchi Jain and Stewart Shuman

Molecular Biology Program, Sloan-Kettering Institute, New York, NY 10065

Table S1

Figures S1, S2, S3

Table S1

Phylogenetic distribution of the bacterial Hen1-Pnkp “RNA repair” cassette

| Species | Hen1 (aa) | Pnkp (aa) | Phylum |
|---|---|---|---|
| Clostridium thermocellulum | 465 | 870 | Firmicutes |
| Actinosynnema mirum | 455 | 834 | Actinobacteria |
| Catenulispora acidiphila | 511 | 870 | Actinobacteria |
| Clavibacter michiganensis | 465 | 861 | Actinobacteria |
| Corynebacterium amycolatum SK46 | 433 | 822 | Actinobacteria |
| Frankia alni str. ACN14A | 480 | 900 | Actinobacteria |
| Gordonia bronchialis | 443 | 852 | Actinobacteria |
| Kineococcus radiotolerans | 480 | 863 | Actinobacteria |
| Kribbella flavida | 478 | 843 | Actinobacteria |
| Micromonospora sp. ATCC 39149 | 494 | 840 | Actinobacteria |
| Nakamurella multipartita | 468 | 852 | Actinobacteria |
| Nocardiopsis dassonvillei | 534 | 864 | Actinobacteria |
| Rhodococcus erythropolis PR4 | 474 | 847 | Actinobacteria |
| Rhodococcus erythropolis SK121 | 467 | 847 | Actinobacteria |
| Rhodococcus opacus B4 | 495 | 845 | Actinobacteria |
| Stackebrandtia nassauensis | 535 | 847 | Actinobacteria |
| Streptomyces albus | 512 | 859 | Actinobacteria |
| Streptomyces avermitilis | 495 | 848 | Actinobacteria |
| Streptomyces clavuligerus | 521 | 848 | Actinobacteria |
| Streptomyces coelicolor A3(2) | 531 | 842 | Actinobacteria |
| Streptomyces ghanaensis | 489 | 855 | Actinobacteria |
| Streptomyces griseus | 497 | 860 | Actinobacteria |
| Streptomyces roseosporus | 502 | 862 | Actinobacteria |
| Streptomyces sp. SPB74 | 525 | 883 | Actinobacteria |
| Streptomyces sviceus | 492 | 847 | Actinobacteria |
| Streptosporangium roseum | 505 | 847 | Actinobacteria |
| Tsukamurella paurometabola | 475 | 830 | Actinobacteria |
| Candidatus Koribacter versatilis | 465 | 850 | Acidobacteria |
| Chitinophaga pinensis | 465 | 847 | Bacteroidetes |
| Microscilla marina | 465 | 858 | Bacteroidetes |
| Herpetosiphon aurantiacus | 460 | 854 | Chloroflexi |
| Anabaena variabilis | 461 | 858 | Cyanobacteria |
| Nodularia spumigena CCY 9414 | 460 | 858 | Cyanobacteria |
| Nostoc sp. PCC 7120 | 460 | 858 | Cyanobacteria |
| Synechococcus sp. PCC 7335 | 475 | 872 | Cyanobacteria |
| Gemmata obscuriglobus | 466 | 877 | Planctomycetes |
| Bradyrhizobium sp. BTAi1 | 459 | 852 | Proteobacteria |
| Bradyrhizobium sp. ORS278 | 468 | 852 | Proteobacteria |
| Maricaulis maris MCS10 | 469 | 852 | Proteobacteria |
| Sorangium cellulosum | 499 | 855 | Proteobacteria |

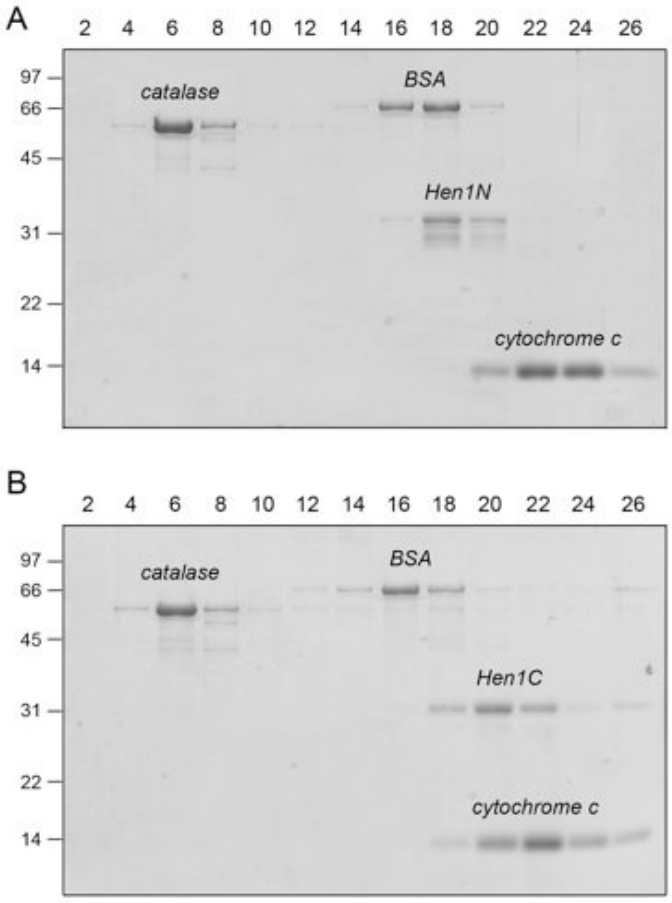


Figure S1. Glycerol gradient sedimentation of the *Cth*Hen1 N- and C-terminal domains.

Zonal velocity sedimentation was performed as described under Methods. Aliquots (15 µl) of even-numbered glycerol gradient fractions of *Cth*Hen1(1-258) (Hen1N, panel A) or *Cth*Hen1(259-465) (Hen1C, panel B) cosedimented with marker proteins were analyzed by SDS-PAGE. The Coomassie-blue stained gels are shown. The Hen1, catalase, BSA, and cytochrome *c* polypeptides are indicated. Molecular weight calibrations for the PAGE analysis (kDa) are indicated on the *left*.

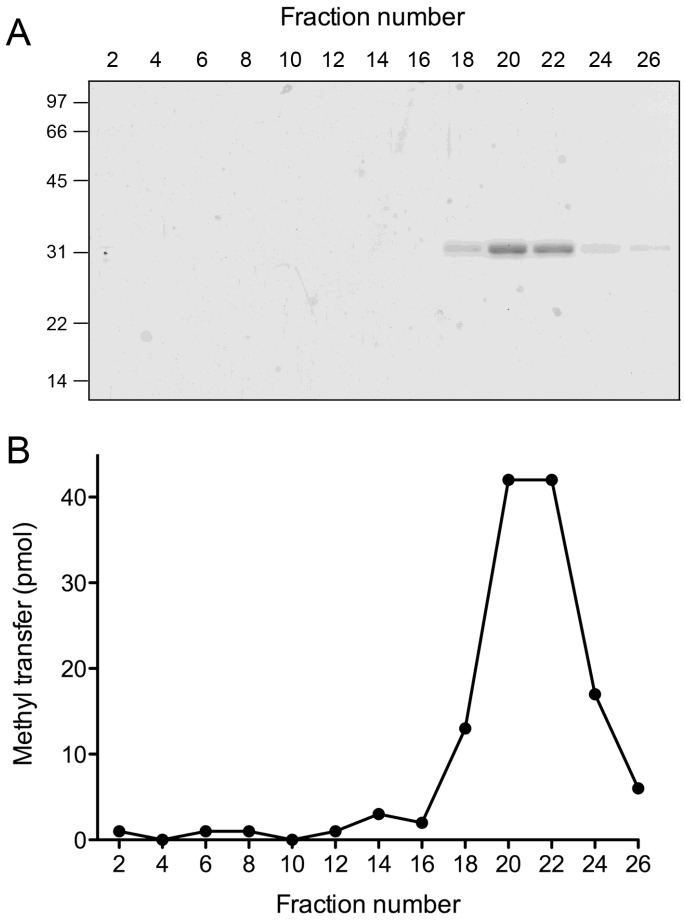


Figure S2. Sedimentation profile of the *Cth*Hen1 C-domain methyltransferase activity.

Zonal velocity sedimentation was performed as described under Methods. Aliquots (15 µl) of even-numbered glycerol gradient fractions of *Cth*Hen1(259-465) sedimented by itself were analyzed by SDS-PAGE. The Coomassie-blue stained gel is shown in panel A. Molecular weight calibrations for the PAGE analysis (kDa) are indicated on the *left*. The methyltransferase activity profile for the glycerol gradient is shown in panel B. Reaction mixtures (10 µl) containing 25 mM Tris-HCl (pH 8.5), 1 mM $MnCl_2$, 20 µM [$^3$H-$CH_3$]AdoMet, 10 µM 24-mer RNA, and 2 µl of the indicated gradient fraction were incubated for 60 min at 45˚C. The extents of $^3$H-methyl transfer to RNA are plotted.

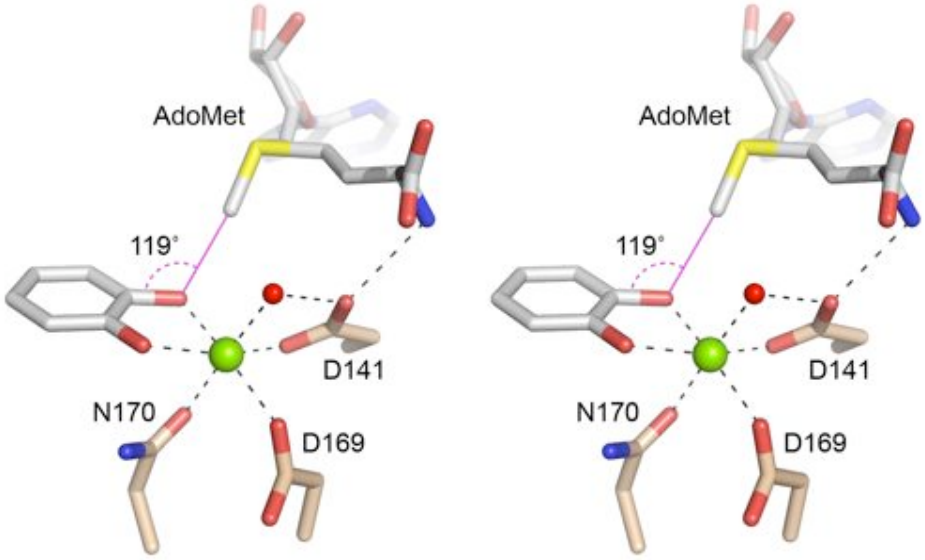


Figure S3. Insights to *Cth*Hen1 mechanism from the structure of catechol O-methyltransferase. Stereo view of the active site taken from the crystal structure (pdb 1VID) of rat COMT bound to AdoMet, $Mg^{2+}$ (green sphere), and a catechol analog inhibitor. The image highlights the octahedral metal coordination complex formed by two aspartates, one asparagine, one water (red sphere), and both vicinal hydroxyls of the catechol ring. The catechol oxygen nucleophile is poised for an in-line attack on the AdoMet methyl carbon. The metal-binding Asp169 residue, which also coordinates the AdoMet amine, is located within a peptide motif of COMT ($^{139}$FLDHW) that is conserved in *Cth*Hen1 ($^{367}$VIEHL) and its eukaryal homologs.